Arabian Journal of Geosciences (2021) 14: 1338
https://doi.org/10.1007/s12517-021-07688-x

ORIGINAL PAPER

Temporal dynamics of primary productivity in the north-eastern Arabian Sea: an evaluation of ocean color models

Vinaya Kumar Vase[1,2] · Nakhawa Ajay[1] · Rajan Kumar[1] · Sreenath Ramanathan[1] · Jayasankar Jayaraman[1] · Prathibha Rohit[1,2]

Received: 30 May 2020 / Accepted: 21 June 2021 / Published online: 7 July 2021

Abstract

We examined the spatial and temporal variations in monthly primary productivity (PP; mg C m^{-2} day^{-1}) in the northern Arabian Sea from 2015 to 2017 using the PP model (Vertically Generalized Production Model, VGPM) to identify and tag productivity zones and seasons. The major objective was to validate the existing satellite algorithms and compare them with the regional parameterization and further define the most accurate model for the region. The models use both in-situ chlorophyll-*a* (Chl-*a*), SST, and euphotic depth (Z_{eu}) (derived from Chl-*a*), and satellite-retrieved (photosynthetically available radiance, PAR and day length, DL) variables as input parameters. The measured PP values showed significant intra-annual variations, and the maximum was during December (3689.2 ± 505.3 mg C m^{-2} day^{-1}) and the minimum during August (2207.7 ± 202.2 mg C m^{-2} day^{-1}). The linear regression depicted that the input variables (Chl-*a*, PAR, Z_{eu}, DL) together explained 48.68% variation in the PP. The chlorophyll-*a* showed significant variability in PP, followed by DL, PAR, and Z_{eu}. We tested three modified models with minor modifications in input variables of basic VGPM. Among the models validated in the region, the VGPM-KI could explain 38.3% of the variance with the in-situ PP data, followed by other models (range of variance explained from 18.7 to 38.3%). The average model precision, as determined by RMSD and the bias, was lowest for the modified model (VGPM-KI, VGPM-BF, and VGPM-E), but highest in case of models with satellite as a sole source of input variables (VGPM and EVGPM). In the northern Arabian Sea, VGPM-KI and VGPM-E performed better than the other models. However, VGPM-KI overestimated the PP values when compared to in-situ estimates. The biogeochemical cycles and ocean processes like coastal upwelling and winter convection by winds, which are the key determiners for perennial productivity in the region, will also affect PP in the region.

Keywords Satellite ocean color · Primary productivity · Models · Validation approach · Northern Arabian Sea

Introduction

The global oceans account for more than half of the Earth's carbon absorbed by photosynthesis and are also known for their role in carbon sequestration and as an integral part of the marine food webs. The marine primary productivity is the proxy to global carbon budget analysis, whose proper estimation will give insights in ecosystem productivity at temporal and spatial scales. Primary production (PP), represented mainly by the marine phytoplankton in the ecosystem, is a source of energy, which supports biological and fishery productivity. The PP in a marine ecosystem are not static, rather varies both in space and time. The variability in PP is mainly influenced by environmental conditions like light radiation, depth, nutrients, mixing processes, and sea surface temperature (SST). The organic matter synthesis of marine phytoplankton through the process of photosynthesis forms the base of energy flow through trophic chain in the marine ecosystem. The process of PP not only fuels biological growth and fish productivity, but also regulates carbon uptake and release by the ocean (Falkowski 1988). Hence, primary production is the base of the marine food chain and acts as a vital entity in the biogeochemical cycles in the ecosystem (Morel and Antoine 2002). The ability to estimate the PP at higher temporal and

Responsible Editor: Haroun Chenchouni

✉ Vinaya Kumar Vase
v.vinaykumarvs@gmail.com

[1] ICAR - Central Marine Fisheries Research Institute, North, P.O., Ernakulam, Kerala Kochi-682 018, India

[2] Mangalore University, Mangalagangotri 574 199, Karnataka State, India

spatial scales has been revolutionized because of the ocean color remote sensing, besides the data provided by in-situ techniques (Eppley et al. 1987; Joo et al. 2016). The chlorophyll-*a* concentration could be accurately computed using ocean color remote sensing satellite, wherein the optical properties are controlled mostly by phytoplankton and other factors like color dissolved organic matter (CDOM) and sediments (Murakami et al. 2006). Primary production can be determined from the satellite-derived data, i.e., surface chlorophyll, SST, and photosynthetically active radiation (PAR) (Longhurst et al. 1995). Several models and parameters have been proposed to estimate vertically integrated primary production (Behrenfeld and Falkowski 1997a; Campbell et al. 2002; Carr et al. 2006).

The ocean color data generates many products to understand the dynamics and prediction of primary production for case 1 and case 2 waters. The standard algorithms engaged in estimation of water-column primary production using photosynthesis-irradiance relationships and rely on remotely sensed chlorophyll-a, light attenuation, and estimated surface irradiance. In case 1 waters, light attenuation in the water column was reasonably well acceptable as a function of chlorophyll-a concentration. In case 2 waters, the computation of light attenuation was not accurate due to suspended sediments and dissolved organic matter as well (IOCCG 2000). The case II waters are in the vicinity of the coastal region (approximately 20–30 m depth) and are more optically complex and dynamic in productivity due to the organic and inorganic constituents in the ecosystem and also for the typical bio-geochemical processes (Vase et al. 2018). But the case II waters are known for its productivity in the oceans because of the shallow depths, light penetration, intense photosynthetic activity, and proper mixing of nutrients and organic matter. Attaining reliable PP measurements by satellites is often tricky in the coastal case II waters due to the complex optical constituents (sediments, CDOM, organic debris, land influences, etc.). Fortunately, the emerging remote sensing techniques have enabled long-term and broad-scale monitoring of PP in the global waters. Various satellite models will yield a range of results, depending mainly on the input parameters and range of uncertainties/limitations of the region. Therefore, the satellite-derived models should consider the peculiarities of regional ecosystems to get good matchups of PP with in-situ observations. The surface primary productivity was influenced by low-salinity river water along with the year through mechanisms associated with the western tropical Atlantic circulation and vertical mixing (Gouveia et al. 2019).

In contemporary literature, a variety of satellite-derived models like WIDI (wavelength- and depth-integrated), WI (wavelength-integrated), semi-empirical were proposed for the estimation of PP in different regions and ecosystems by considering the variability in photosynthetic efficiency on hydro-optical and biochemical conditions (Behrenfeld et al. 2006; Smyth et al. 2005). In general, the ocean color models differ in both their type (carbon-based versus chlorophyll-based) and complexity (depth- and wavelength-integrated versus resolved). The modern method to estimate the large-scale PP is to use coupled biogeochemical (BG) marine numerical models, which provide the large-scale daily estimates of PP by running at appropriate horizontal and vertical resolutions. The BG models parameterize photosynthesis similar to the satellite PP algorithms. Still, the fundamental difference between these two approaches, however, is that satellite algorithms require satellite estimates of surface chlorophyll and temperature as input variables (McClain 2009). In contrast, BG models explicitly compute these fields (Gregg 2008). Recently, the abilities of 36 models were evaluated to estimate the decadal trends in NPP at two time-series stations in the North subtropical gyres of the Atlantic and Pacific Oceans (Saba et al. 2010). The Vertically Generalized Production Model (VGPM) verified by the in-situ primary production data explained only 40% of the variability in the Sagami Bay, Japan. The in-situ measurements during cloudy days point out that the use of satellite data, which is restricted to sunny days, overestimates primary production (Ishizaka et al. 2007). Accurate PP estimates are crucial to understand the global carbon cycles and many of the critical oceanic processes. However, it is imperative to validate the performance of the various PP algorithms with in-situ/ship born observations to explain the reasons underlying the similarities/differences in model outputs. Many such comparisons were carried out recently as a part of the Primary Productivity Algorithm Round Robin (PPARR) series funded by NASA (Campbell et al. 2002; Carr et al. 2006; Friedrichs et al. 2009; Saba et al. 2011).

Globally, over twenty models are in use for estimation of the PP, and most of them use remotely sensed data for the diverse ocean ecosystems. A few of these models have been validated to find out their relative or absolute accuracy (Platt et al. 1991; Behrenfeld and Falkowski 1997b; Campbell et al. 2002; Kameda and Ishizaka 2005; Carr et al. 2006; Friedrichs et al. 2009; Saba et al. 2010; Saba et al. 2011; Tilstone et al. 2015; Lobanova et al. 2018; Regaudie-de-Gioux et al. 2019) (Table 1). Usage of satellite-derived model input parameters (Chl-a, PAR, SST, etc.) may lead to an inaccurate estimation of PP when compared to the local field measurements (Campbell et al. 2002). The in-situ values were used as input parameters in the algorithms to arrive at accurate measurements in the present study. Experimental cruise-based estimates of PP over larger spatial and temporal scale are limited. As a result, continuous and long-term PP studies for the northern Arabian Sea are rare. Various researchers studied the seasonal variations in physical and chemical characteristics, nutrient dynamics in the network of coastal, and offshore waters across the country (Mathew and Pillai 1990; Manikannan et al. 2011; Temkar et al. 2015; Vase et al. 2018). The major objective of this study was to compare the in-situ PP

Table 1. Measurement and validation of satellite-based ocean color primary productivity models across the global regions

Ecosystem type	Region of study	Period of study	Primary production (mg C m^{-2} day^{-1})	Model skill (test statistics)	Reference
Subtropical	Northwest Atlantic Ocean	1989	978 ± 235	RMSD 0.15 ± 0.07	Doney et al., 1996
Temperate	Northeast Atlantic Ocean	1993–1999	535 ± 313	RMSD 0.33 ± 0.08	Doney et al., 2007
Subtropical	Northwest Atlantic Ocean–Sargasso Sea	1988–2003	460 ± 199	RMSD 0.34 ± 0.09	Saba et al. 2010
Temperate	Black Sea	1992–1999	341 ± 197	RMSD 0.44 ± 0.09	Kara et al., 2005
Temperate	Mediterranean Sea	1990–2007	658 ± 639	RMSD 0.42 ± 0.06	D'Ortenzio et al., 2005
Tropical	Arabian Sea	1995	1075 ± 373	0.22 ± 0.09	Saba et al. 2011
Subtropical	North Pacific Ocean	1989–2005	489 ± 149	RMSD 0.26 ± 0.07	Friedrichs et al. 2009
Temperate	Japan Sea	1998–2002	191	R^2 = 0.967	Yamada et al. 2005
Tropical-subtropical rim	South China Sea	1998–2006	300	R^2 = 0.705 RMSE = 76.45	Tan and Guang-Yu 2009
Polar	Southern Ocean	1996–2006	1274 ± 812	RMSD 0.33	Arrigo et al. 2008
Temperate	Baltic sea	2008–2011	--	R^2 = 0.38	Malgorzata and Agata 2013
Tropical	Sagami Bay, Japan	1999–2003	168–1961	R^2 = 0.434	Ishizaka et al. 2007
Temperate	Northeast Atlantic Ocean	1998–2013	500–1500	r = 0.66 RMSE = 0.56	Lobanova et al. 2018
Tropical/subtropical	Sub-tropical gyre	2010–2011	125 ± 62 to 434.6 ± 193.5	R^2 = 0.07 to 0.53	Regaudie-de-Gioux et al. 2019

measurements with the five PP models (two satellite-based and three modified variants of VGPM). Besides, the study also proposes the most reliable model to estimate PP in the region by improving the understanding of the similarities and differences between the different models. The comparative results between the models attempted in the present study will also interest other researchers who aspire to execute satellite estimates of PP in the region. The in-situ PP measurements used to validate the modeled output to apply the effect of the modified model in the northern Arabian Sea.

Methodology

Study area and sampling period

The Arabian Sea is one of the most productive oceans compared to any other ocean in the world (De Sousa et al. 1996) (Figure 1a). The region is known for its high nutrient levels, light intensity, inflow of important nutrients from river runoff and Aeolian dust, and consistently higher temperature. The oceanographic processes like coastal upwelling during the southwest monsoon and convective mixing because of the surface winds during winter maintain higher productivity in the study region (Vase et al. 2018). Samples were collected from four different sampling stations perpendicular to the coast up to 75 m depth, which comprised both case I and case II waters. Vessel-based PP measurements covering two sampling locations, i.e., off Veraval (N = 100) and Okha (N = 104) coasts along the northern Arabian Sea, were collected (Figure 1b, 1c, and 1d) for 3 years (2015 to 2017). A total of 204 samples were analyzed from different locations during the winter monsoon (N = 96) (November–February), spring inter monsoon (N = 56) (March–May), summer monsoon (N = 28) (June–September), and fall inter-monsoon (N = 24) (October) to understand the seasonal variations in PP (DAHDF 2011). Rough sea conditions during the peak monsoon months (June–July) prevented sampling during this period.

In-situ sampling

The sea surface temperatures were measured using a mercury thermometer and CTD probe simultaneously. In order to estimate chlorophyll-*a*, samples collected from the different sampling stations were allowed for filtration through 47 mm GF/F filter paper. The filter paper was placed in a 90% acetone solution and kept in darkness for 24 h in a refrigerator. The extracted material was separated using a centrifuge (R 24 Research Centrifuge, REMI, India), and its absorbance concentration was calculated using a spectrophotometer (EPOCH2TC Micro-plate reader, Biotech, USA) at different wavelengths 750 nm, 665 nm, 645 nm, and 630 nm (Vase et al. 2018).

Historically, several methods such as radiolabeled carbon, rapid fluorescent-based, and O_2/Ar ratio methods (Strickland and Parsons 1968; Peterson 1980; Boyd et al. 1997; Lobanova et al. 2018) were used for estimation of PP in marine ecosystems. For the present study, the in-situ primary production was

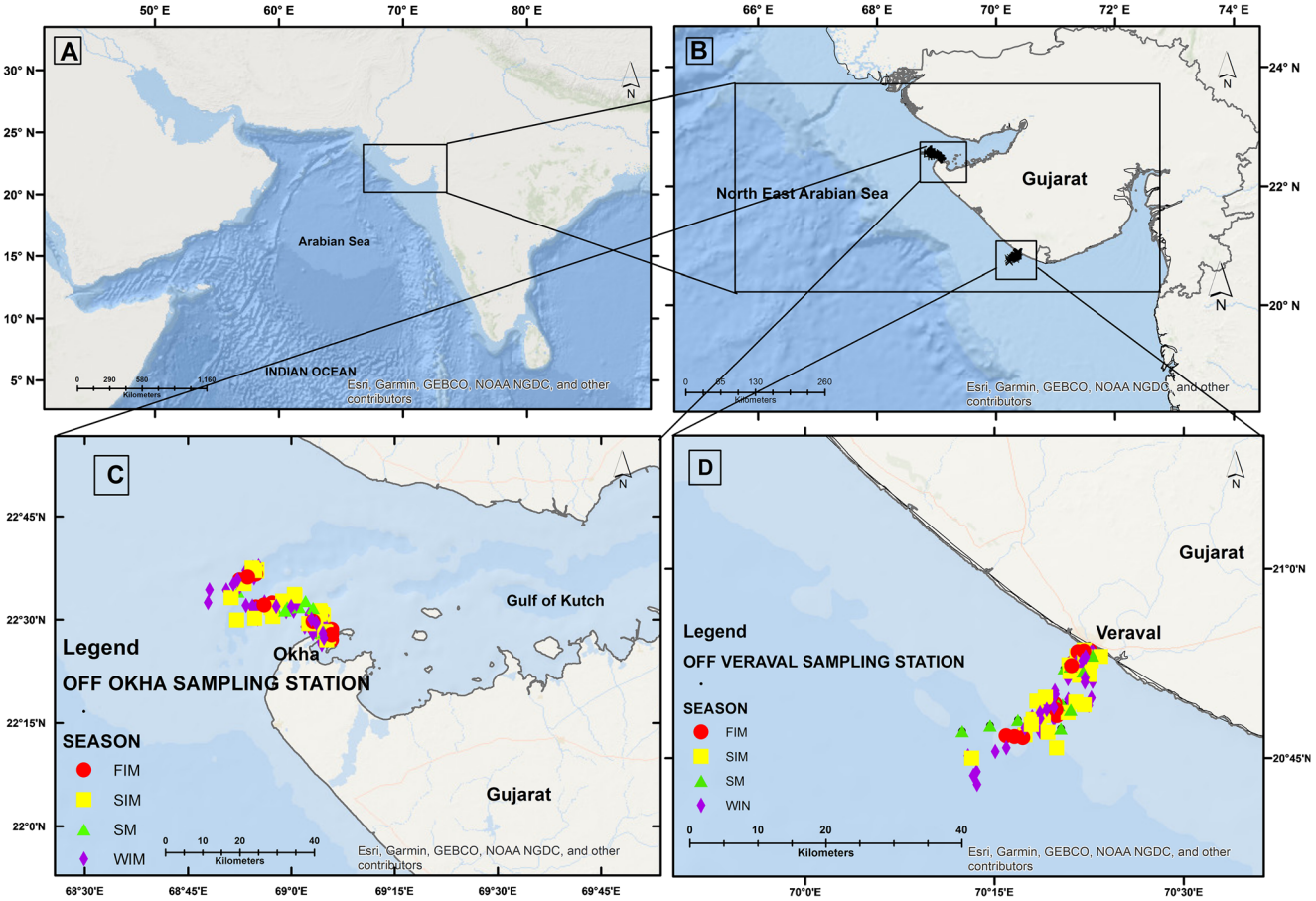

Figure 1. Map of the study area, i.e., **a** the Arabian Sea, **b** the northern Arabian Sea off Gujarat, **c** off Okha coast, **d** off Veraval coast with sample locations of the 204 in-situ PP measurements among two sampling stations during 2015–2017

measured by the Light and Dark bottle method with 3-h incubations for stations S1, S2, S3, and S4. The water samples were incubated for a suitable time at controlled illumination and temperature (providing in-situ conditions). The water samples (300 ml) for the dissolved oxygen (DO) estimation were collected from just beneath the sea surface during 09:00 to 14:00 h of the sampling day. The estimates of DO from replicates were very comparable and robust (SE < 0.05) and hence found suitable for the estimation of NPP. The changes in dissolved oxygen levels in the light bottles were expressed as productivity in g C/unit volume/h and calculated as given below (Gaarder and Gran 1927; Strickland and Parsons 1968).

$$NPP = \frac{(x-z) \times 0.536}{PQ \times t} \text{ mg C/l/hr}$$

where x is O_2 of the light bottle after incubation, z is O_2 of light bottle initially fixed, PQ is the photosynthetic quotient (1.25), and "t" is the number of hours of incubation (3 h). The 0.536 is conversion factor, which defines 1 ml O_2 released by photosynthesis is equivalent to 0.536 mg C. The above value should be multiplied by 10000 (assuming ten sunshine hours affecting photosynthesis in a day) for the expression of productivity in m^{-3} day^{-1}. Though 14C method is more preferred, reasonable results can be attained using Light and Dark bottle method for the estimation of PP validation (Lan et al. 2020).

Satellite data

Remotely sensed PP data (VGPM) from 2015 to 2017 was used to understand the spatial and temporal variation in the northern Arabian Sea (20–24°N, 66–72°E). The 8-day composite level 3 satellite data were retrieved from the OC-CCI (Ocean Colour-Climate Change Initiative) database version 1 (Peters et al. 2019). The database was of chlorophyll-a concentration, and the downwelling diffuse attenuation coefficient at 490 nm was from the SeaWiFS and MODIS. The PAR (8-day composite and level 3 data) was retrieved from the Ocean Productivity (NASA's OceanColor Web) database (O'Malley 2019). The composite images had a spatial resolution of 4 × 4 km. For the calculation of Z_{eu}, and the downwelling diffuse attenuation coefficient at 490 nm (k_d) was used. But, the satellite-derived k_d is a highly variable parameter for the uncertainties in light penetration and reflection. Instead of k_d, an in-situ Chl-*a* data was used in the

estimation of Z_{eu} to minimize the error. The day length (DL) is a synonym of photoperiod (h) and was calculated using an astronomical algorithm as a function of a latitude and a day for a year (O'Malley 2019; Thorsen 2019). The euphotic depth (Z_{eu}) is a function of parameters like k_d and surface chlorophyll, which can be used independently to estimate the same. The Z_{eu} can be estimated with parameter k_d at 490 nm using the following equation, considering the radiation at euphotic depth as 1% of what is available at the surface (Morel et al. 2007).

$$Z_{eu} = \frac{\ln(100)}{k_d} = \frac{4.6}{k_d}$$

where k_d is the downwelling diffuse attenuation coefficient of solar radiation in water (m^{-1}).

Depth of the euphotic zone (Z_{eu}) is the depth where E_0 decreases to 1%, which is estimated by surface chlorophyll (Chl-a_{sat}) using the following equation (Morel and Berthon 1989).

$$C_{tot} = \left\{ \begin{array}{l} 38.0\ (C_{sat})^{0.425}\ when\ C_{sat} \leq 1.0 \\ 40.2\ (C_{sat})^{0.507}\ when\ C_{sat} > 1.0 \end{array} \right\}$$

$$Z_{eu} = \left\{ \begin{array}{l} 568.2\ (C_{tot}) - 0.746\ when\ Z_{eu} \leq 102 \\ 200.0\ (C_{tot}) - 0.293\ when\ Z_{eu} > 102 \end{array} \right\}$$

where C_{sat} is the surface chlorophyll (mg m^{-3}) and C_{tot} is the total chlorophyll (mg m^{-3}).

The third approach used to estimate the Z_{eu} was by considering chlorophyll (Chl in mg m^{-3}) as an input variable in the algorithm suggested by Ishizaka et al. (2007).

$$Zeu = \frac{1}{(0.0186 + 0.0072 \times Chl)}$$

In the present study, the second and third approaches yielded similar Z_{eu} estimates deviating from the first approach, which was calculated using k_d as an input variable. The Z_{eu} estimates by chlorophyll as input parameters were more reliable, and with minimum variance, hence, adopted in the VGPM equations.

Primary production models

The PP in the Arabian Sea from 2015 to 2017 was estimated using five different approaches, namely VGPM (Behrenfeld and Falkowski 1997a, 1997b), Vertically Generalized Production Model with Eppley parameterization (EVGPM, Eppley 1972), and three modified versions of VGPM models. The estimates from the first two methods are solely based on satellite-retrieved input parameters, whereas the modified VGPM models incorporate in-situ estimates of SST, chlorophyll a (Chl), and euphotic depth (Z_{eu}). The updated model, VGPM-BF estimates P^{B}_{opt} (maximum primary production per unit of chlorophyll in the vertical profile) using function of Behrenfeld and Falkowski 1997a, 1997b). The modified models, VGPM-E and VGPM-KI estimates P^{B}_{opt} based on Eppley (1972) and Kameda and Ishizaka (2005), respectively (Figure 2). The intake of satellite-derived chlorophyll-*a* as an input parameter in the algorithm of optically complex case II water may lead to erroneous PP estimates (error multiplication). The in-situ Chl-*a* was more appropriate as an input data for the improvement of the algorithm to avoid the poor performance of ocean color models in the region. In the present study, we also theorized that the integrated primary production estimates by ocean color satellite data (VGPM and EVGPM) with adjusted model parameters (chlorophyll-*a*) are better and comparable to in-situ primary production.

PP Model 1: Satellite Vertically Generalized Production Model (VGPM)

The VGPM, a standard MODIS algorithm, developed by Behrenfeld and Falkowski 1997a, 1997b) (Campbell et al. 2002), is one of the most widely known and used WIDI (wavelength- and depth-integrated) PP models. The model estimates daily primary production in the euphotic layer from total Chl-*a* concentration, PAR, day length, euphotic depth, and the optimum photosynthetic rate (P^{B}_{opt}) of phytoplankton in the water column. In general, the euphotic depth was estimated using K_d in most of the algorithms. The VGPM proposed by Behrenfeld and Falkowski (BF) is as follows:

$$IPP = 0.66125 \times P^{B}_{opt} \times \left[\frac{PAR}{(PAR + 4.1)}\right] \times Z_{eu} \times Chl \times D_{irr}$$

where IPP, P^{B}_{opt}, PAR, Z_{eu}, Chl-*a*, and D_{irr} are integrated primary production (mg C m^{-2} day^{-1}), maximum primary production per unit of chlorophyll in the vertical profile (mg

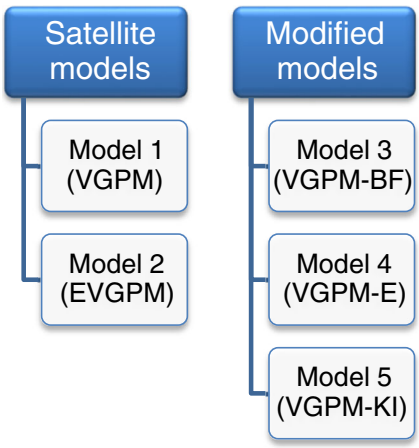

Figure 2. Schematic diagram of different PP models adopted in the current study

C m^{-2} h^{-1}), photosynthetically active radiation (mol quanta m^{-2} day^{-1}), depth of euphotic zone (m), sea surface chlorophyll (mg m^{-3}), and day length (h), respectively.

P^B_{opt} is expressed by BF as a 7th-order polynomial of temperature (T):

$$P^B_{opt} = -3.27 \times 10^{-8} T^7 + 3.4132 \times 10^{-6} T^6 - 1.348 \times 10^{-4} T^5 + 2.462 \times 10^{-3} T^4 - 0.0205 T^3 + 0.0617 T^2 + 0.2749 T + 1.2956$$

PP Model 2: Vertically Generalized Production Model with Eppley parameterization of the temperature effect (EVGPM)

This model estimates P^B_{opt} as an exponential function of the water temperature, which is deviating factor from the VGPM (model 1) (Eppley 1972). The temperature functions are often used to set the upper limit of phytoplankton growth rates in the dynamic ecosystem production models. One temperature function commonly used is that developed by Eppley:

$$P^B_{opt} = 0.59 e^{0.0633T}$$

The Eppley P^B_{opt} was defined in the VGPM equation by Behrenfeld and Falkowski 1997 as:

$$P^B_{opt} = 1.54 * 10^{(0.0275 * T - 0.07)}$$

This exponential relationship defines the maximum attainable daily growth rate (P^B_{opt} d^{-1}) of phytoplankton as a function of temperature (T, °C) and has the advantage over more complex functions. The P^B_{opt} was computed in the present study was as per equation proposed by Behrenfeld and Falkowski 1997a, 1997b). Eppley indicated that the data fell within an upper envelope and drew a line by eye that defines the maximum expected growth at any given temperature between 0 and 40 °C (Eppley 1972).

PP Model 3: Modified Vertically Generalized Production Model (VGPM-BF)

The key input parameters in the VGPM model were replaced with the in-situ variables to check the skill performance of the model. The estimation of primary productivity in this model depends largely on the empirical relationship between SST and P^B_{opt}, represented by a seventh-order polynomial function. Considering the problem, the P^B_{opt} was calculated using in-situ SST instead of satellite-derived SST. In the case of VGPM (model 1), the euphotic depth was estimated using K_d, which is a highly fluctuating parameter. Hence, to avoid the error multiplication, in-situ chlorophyll was used in the calculation of Z_{eu} (Ishizaka et al. 2007; Morel and Berthon 1989).

PP Model 4: Modified Vertically Generalized Production Model with Eppley parameterization of the temperature effect (VGPM-E)

The P^B_{opt} in the algorithm was estimated using in-situ SST as an exponential function to reduce the error. Euphotic depth was measured using in-situ chlorophyll instead of k_d, and the PAR was retrieved from satellite data. The key productivity parameter chlorophyll was measured in-situ.

PP Model 5: Modified Vertically Generalized Production Model by Kameda and Ishizaka (VGPM-KI)

The P^B_{opt} formulate as a function of SST and Chl-a in this VGPM variant (Kameda and Ishizaka 2005). The model relies on the assumption that the chlorophyll-specific productivity is inversely proportional to phytoplankton size. Kameda and Ishizaka modified the P^B_{opt} according to the under-given equation, assuming small and large phytoplankton communities, both with 3rd-order polynomial temperature dependency. Besides, the phytoplankton communities (the smaller one) have constant biomass.

$$P^B_{opt} = \left(0.017T - 3.2 \times 10^{-3} T^2 + 3.0 \times 10^{-5} T^3\right)/Chl + \left(1.0 + 0.17T - 2.5 \times 10^{-5} T^2 - 8.0 \times 10^{-5} T^3\right)$$

where Chl-a (chlorophyll-a concentration in mg m^{-3}) and SST used in the equation were in-situ. The daily averaged surface photosynthetic active radiation at 400–700 nm (PAR) (E m^{-2} day^{-1}) was remotely sensed, and other input parameters like Z_{eu} (Ishizaka et al. 2007) used in the algorithm were measured.

Model performance

Descriptive statistics were calculated for the different input variables and also for the PP measurements estimated from the various models. Temporal variations in in-situ chlorophyll and primary productivity measurements were analyzed to understand the productivity cycles in the region. The mean absolute percentage error (MPE) was calculated for understanding how close are the model predictions (P_n) to the in-situ observations (O_n) using the following formula (Malgorzata and Agata 2013):

$$MPE = 100 \frac{1}{N} \sum_{n=1}^{N} \left| \frac{P_n - O_n}{O_n} \right|$$

Another precision indicator, RMSD (root mean square difference), was used to assess model efficiency. The root mean square difference (statistical error) was estimated to assess overall model performance in terms of both bias and variability in a single statistic. The RMSD assesses model skill such that models with lower values had higher efficiency (Saba et al. 2010):

$$RMSD = \left(\frac{1}{N}\sum_{i=1}^{N}\Delta(i)^2\right)^{1/2}$$

where the model-data misfit in $\log_{10}$ space $\Delta(i)$ is defined as:

$$\Delta(i) = log(NPP_m(i)) - log(NPP_d(i))$$

and $NPP_m(i)$ is modeled NPP, and NPP_d (i) represents in-situ data for each sample 'i'. In order to assess the model skill more specifically (whether a model over- or underestimated NPP), we calculated each model's bias (B) for each region as:

$$B = \overline{log(NPP_m)} - \overline{log(NPP_d)}$$

One-way analysis of variance (ANOVA) was attempted to assess the significant differences between the model and in-situ mean PP values on temporal and spatial scales. Finally, the scatter diagrams, standard deviation (SD), Pearson's correlation coefficient, and linear regression (coefficients S and I) were considered to understand the consistency between modeled and in-situ PP estimates.

Results

The in-situ primary productivity, PP ranges from 1937.8 to 4863.0 mg C m^{-2} day^{-1} (mean PP was 3372.1 ± 665.1 mg C m^{-2} day^{-1}). The higher in-situ PP was estimated in the month of December (3689.2 ± 505.3 mg C m^{-2} day^{-1}, N = 24) and lower PP was in the month of August (2207.7 ± 202.2 mg C m^{-2} day^{-1}, N = 4). Strong significant temporal variations were observed in in-situ PP concentrations in the region. The one-way ANOVA infers the monthly significant difference (at 95% of significance) in PP ($F(9,194) = 2.35$, $P = 0.015$). The distinct grouping was observed in in-situ PP across different months using a Tukey post-hoc test. Significant temporal variations in model 1 estimate for the region were evident during 2015 to 2017 period (Fig. 2). Noticeable monthly differences were observed in the satellite PP measurements with the maximum recorded in February (2349 ± 231 mg C m^{-2} day^{-1}) and the minimum in June (700 ± 13 mg C m^{-2} day^{-1}) (Figure 3). The ANOVA coefficients and the post-hoc test revealed significant variations in PP measurements between the months (F =1 2.43; $p < 0.005$ and R^2 = 85.07%) in the region. The seasonal variations in satellite PP measurements were observed during different seasons, and the maximum was during the winter monsoon (1722 ± 439 mg C m^{-2} day^{-1}), followed by spring inter-monsoon (1265 ± 648 mg C m^{-2} day^{-1}), fall inter-monsoon (1197 ± 425 mg C m^{-2} day^{-1}), and summer monsoon (991 ± 277 mg C m^{-2} day^{-1}). The ANOVA results inferred the significant variations in PP measurements among different seasons ($F = 5.28$; $p < 0.005$ and R^2 = 33.11%). The Tukey post-hoc test revealed the highest productivity during the winter, in contrast with the summer monsoon having the lowest productivity. The moderate productivity was observed during fall inter-monsoon and spring inter-monsoon seasons in the study region. Inter-annual variation of average primary production was calculated in the region, and the highest variations were recorded in winter (32.63%) and spring (25.63%), followed by fall monsoon (22.81%) and monsoon (18.93%).

In the present study, a key input parameter Z_{eu} was estimated using three approaches. The first one using k_d gives different estimates than the latter two based on chlorophyll. The chlorophyll-based estimates were found more comparable, reliable, and with minimum variance and hence were adopted in VGPM equations. The ranges of input variables (inclusive of satellite and in-situ estimates) used in the models were SST ranged from 22.50 to 28.20 °C (25.74 ± 1.26 °C); PAR from 28.48 to 56.29 Ein m^{-2} day^{-1} (43.24 ± 7.37 Ein m^{-2} day^{-1}); DL from 10.45 to 13.10 h (11.47 ± 0.72 h); Z_{eu} from 23.96 to 43.12 m (32.44 ± 3.70 m); and Chl-*a* ranged from 0.446 to 2.951 mg m^{-3} (1.422 ± 0.44 mg m^{-3}) (Figure 4a and b). The mean input variables showed distinct temporal (monthly) variations in the region. A significant positive correlation (r = 0.79) was observed between monthly mean SST and PAR, whereas a moderate correlation (r = 0.61) was evident between mean chlorophyll-a and estimated primary productivity. In-situ PP estimate also showed variation between the seasons, the highest mean PP values were recorded during winter (3430 mg C m^{-2} day^{-1}), and the lowest were during monsoon season (3129 mg C m^{-2} day^{-1}) (Figure 5).

Among various estimated PP datasets, the highest mean PP was from model 3 (8818.0 mg C m^{-2} day^{-1}), while the lowest PP was from model 1 (1183.60 mg C m^{-2} day^{-1}). The maximum data spread (interquartile range) was observed with modeled PP-BF dataset (2734.0 mg C m^{-2} day^{-1}) and the minimum for the satellite VGPM (664.5 mg C m^{-2} day^{-1}) (Table 2). The MPE values were negative in the case of satellite data sets (− 51.11 for EVGPM and − 64.88 for VGPM), but the values were positive for the modified model (ranges from 56.90 to 166.60). The MPE result indicated that the PP measurements were underestimated by satellite data (EVGPM and VGPM) and overestimated by the modified models (with in-situ data) in the region. The Pearson correlation coefficient (r) varied from 0.43 to 0.62, when comparing the in-situ PP with different modeled PP measurements. The in-situ PP estimates showed a significant positive correlation with modeled

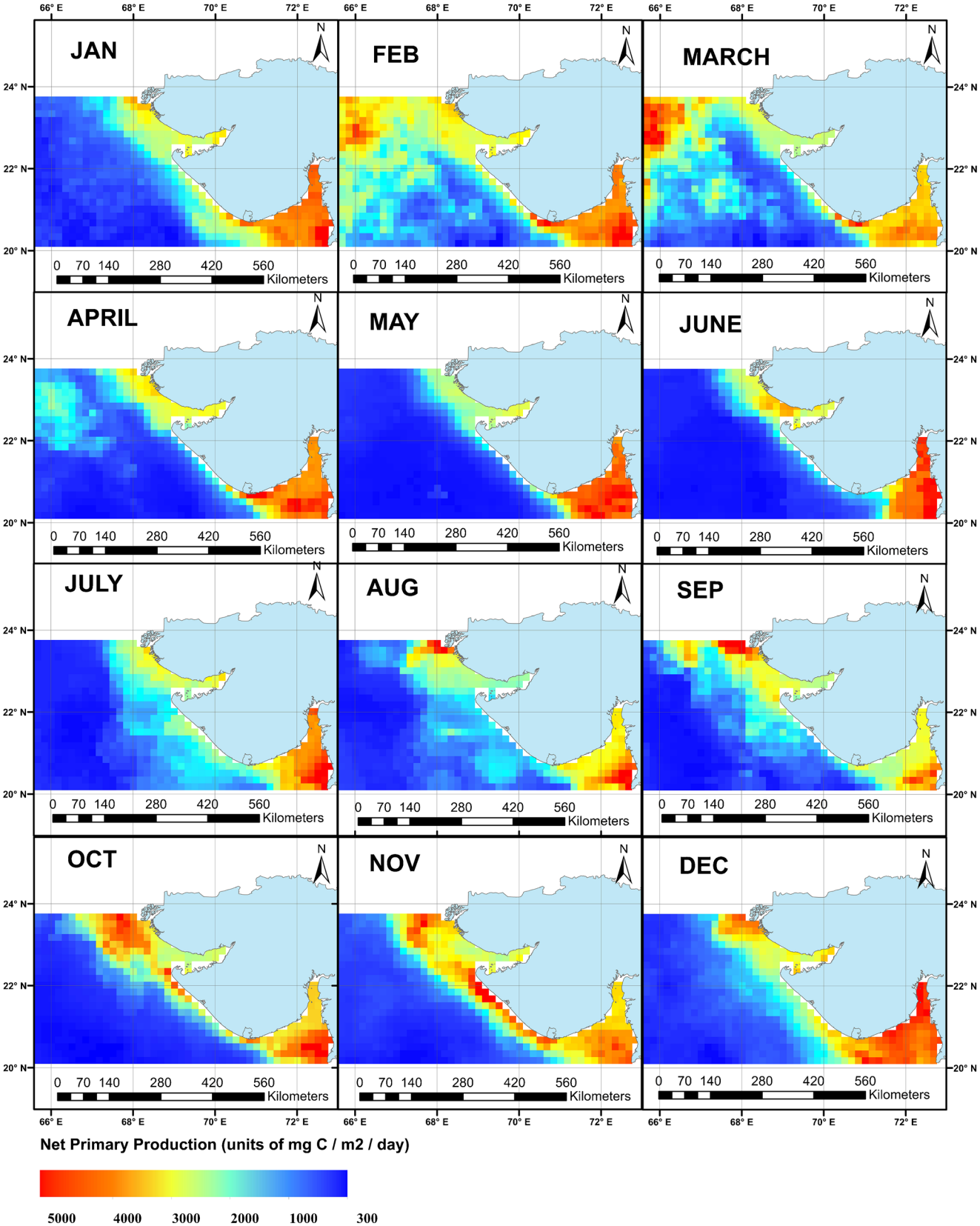

Figure 3. Monthly averaged integrated primary production from 2015 to 2017 estimated by satellite VGPM in the study region, i.e., northern Arabian Sea

PP from model-3 (r = 0.581), model-4 (r = 0.565), and model-5 (r = 0.619). The in-situ PP data showed a fairly significant positive correlation with PP values of model-1 (r = 0.421) and model-2 (r = 0.500) (Figure 6). The RMSD was not consistent among five different models (ranged from 0.02 to 0.14) in the study region. Lower ability was shown by the model 1 while estimating variance of PP due to the high RMSD (0.14). A significantly better skill performance was observed for the modified VGPM variants, i.e., VGPM-E (0.02), VGPM-KI (0.06), and VGPM-BF (0.09). The average RMSD calculated across the five models for the regions is 0.10.

The model is believed to be efficient in its skill, if it can reproduce values in proximity of mean of field observations. The model efficiency (ME) values were − 4.33 in VGPM-E model, followed by VGPM-KI (− 13.05), EVGPM-E (− 15.25), VGPM-BF (− 21.69), and VGPM (− 34.36). The model efficiency (ME) showed significant variations between the models, but none of the models did better than the mean measured data (ME < 0) in the region. The log bias values for the three VGPM variants were overestimates of in-situ PP (VGPM-E is 0.19, VGPM-KI is 0.33, and VGPM-BF is 0.42) as compared to the other two models (VGPM model is − 0.33, and EVGPM model is − 0.49) (Figure 7). VGPM-E was the most accurate in three out of six statistical tests performed because of the parameterization with the input variables. The PP estimates of VGPM-KI proved better for the region, supported by two critical statistical tests (r = 0.619, p < 0.000, and R^2 = 0.383) out of six statistical tests. Overall, the VGPM-E and VGPM-KI models were more accurate in the northern Arabian Sea with minimal statistical errors. Nearly 38.0% of variation was explained by VGPM-KI (R^2 = 0.383) and 34% by VGPM-BF (R^2 = 0.338) with the in-situ PP measurements (Figure 8d and e). Relatively lower variation was explained by VGPM-E (R^2 = 0.319), EVGPM (R^2 = 0.251), and VGPM (R^2 = 0.187) (Figure 8a, 8b, and 8c and Table 3). The RMSD was as low as 0.02 with VGPM-E with measured PP values, which performed better compared to the other models in the region.

Discussion

The real-time dynamics of marine ecosystems on a large scale can be steered in a synoptic manner by using satellite-based ocean color observations. Quantification of oceanic PP with in-situ measurements is much harder, expensive, and time-consuming. Hence, spatial satellite technologies that provide more extensive coverage with less cost of data collection are gaining popularity. Ocean color models were used to assess the contemporary trends in global NPP (Behrenfeld et al. 2006), relationships between sea-ice variability and NPP in the Southern Ocean (Arrigo et al. 2008), bottom-up forcing on leatherback turtles (Saba et al. 2008), and fisheries management (Zainuddin et al. 2006). Though the Arabian Sea is one of the highly productive and supporting vast biota, studies on primary productivity estimation, dynamics, and validation of remotely sensed products are limited (Vase et al. 2018; Saba et al. 2011).

Significant temporal variations (monthly and seasonal) were observed in satellite PP data (VGPM) in the region. The peak primary production was found during winter and spring, with maximum values recorded in February (2329 ± 231 mg C m^{-2} day^{-1}), followed by March (2062 ± 484 mg C m^{-2} day^{-1}). The SST and PAR were found to have a strong bearing on the temporal variation in observed primary productivity. The other factors not included in a present study like nutrients, winter convective mixing by winds, and upwelling could also have a fair share of influence on primary productivity (Pesce et al. 2018). Several factors, notably temperature, solar radiation, and light intensity can delimit the upper bound of primary production when limiting in marine ecosystems, even when other factors, especially nutrient concentrations are conducive (Tan and Guang-Yu 2009). However, the study region is in the tropics, where solar radiation (PAR 28.48 to 56.29 Ein m^{-2} day^{-1}), light intensity (average day length 11.47 h), and temperature (22.50–28.20 °C) are on higher side year-around and are favorable for photosynthesis (Racault et al. 2012). The wide continental shelf and the existence of

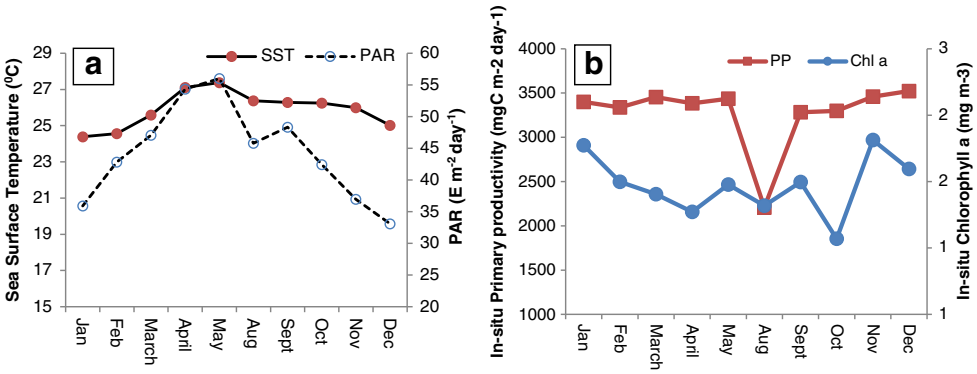

Figure 4. Monthly average variations **a** SST and PAR, **b** Chl-*a* and Primary production

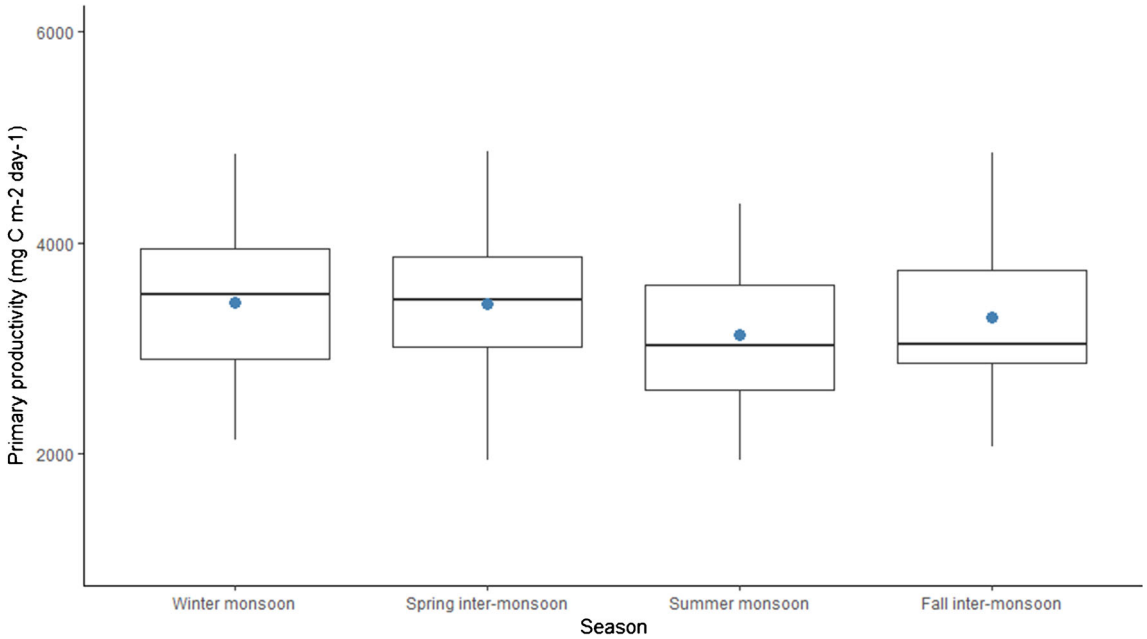

Figure 5. Seasonal variations in in-situ measured PP (N = 204) during 2015–2017 (no samples were collected during the months of June and July).

Gulf ecosystems, winter convective mixing, and coastal upwelling are the key determiners for higher productivity in the region.

Significant differences were observed in the primary production measured using satellite data and in-situ data in the region. The primary production measurements using the satellite data for longer timescale will lead to an overestimation of PP as compared to the daily primary production data (Ishizaka et al. 2007). In a study comparing the ability of seven algorithms to estimate depth-integrated daily PP (mg C m^{-2} day^{-1}) in the Baltic Sea, the modeled and measured PP agreed with the region specific Development of a satellite method for Baltic ecosystem monitoring (DESAMBEM) algorithm (Małgorzata and Agata 2013). Overall, the global remote sensing algorithms significantly overestimated PP in the Baltic Sea, and the DESAMBEM underestimated PP for the most significant values of measured PP. The current study is in agreement with the previous observations that the model values generally overestimate the PP in comparison with the measured PP values. The VGPM model typically overestimated PP in the North Atlantic Drift province (Tilstone et al. 2009). The optimal photosynthetic rate (P^B_{opt}) is a function of SST and the uncertainties in the SST may cause errors while calculating P^B_{opt}. We estimated P^B_{opt} with the in-situ SST as input variable instead of satellite SST to address the error while calculating PP through the VGPM algorithm. Also, the photosynthetic parameter robustly depends on other factors, i.e., nutrient supply, irradiance, and dominant phytoplankton species (Behrenfeld and Falkowski 1997b).

In the case of VGPM, k_d caused the most significant error (Lobanova et al. 2018) while calculating the Z_{eu}. In-situ Chl-*a* was used for the calculation of Z_{eu} to reduce the error associated with k_d (Morel and Berthon 1989; Ishizaka et al. 2007). Ishizaka and Morel and Berthon observed that Z_{eu} estimated by the algorithms incorporating Chl-*a* as an input variable were relatively more accurate (35.17 ± 3.61; CV = 10.26) and (32.47 ± 3.66; CV = 11.29), respectively than the k_d based algorithm (29.03 ± 17.47 and CV = 60.18) (Morel et al. 2007). The P^B_{opt} with VGPM-KI and integrated primary production measurements were reasonably accurate in the Japan Sea (Yamada et al. 2005). Siswanto et al. (2006) also established

Table 2. Descriptive statistics of Primary production (mg C m^{-2} day^{-1}) measured by in-situ and various models in the study region (N = 204)

Type of dataset	Mean	St Dev	Minimum	Maximum	Q1	Q3	IQR	Coef Var
$PP_{in\text{-}situ}$	3372.1	665.1	1937.8	4863.0	2870.9	3903.0	1032.1	19.72
EVGPM	1645.9	602.0	659.9	3614.7	1277.0	2030.4	753.4	36.6
VGPM	1183.6	514.4	312.6	2669.2	790.2	1454.7	664.5	43.5
VGPM-KI	7099.9	1295.2	4545.9	11029.0	6160.3	7882.6	1722.3	18.2
VGPM-BF	8799.0	1779.0	5355.0	14369.0	7373.0	10060.0	2687.0	20.2
VGPM-E	5181.5	1130.0	2838.1	8713.1	4410.7	5706.1	1295.4	21.8

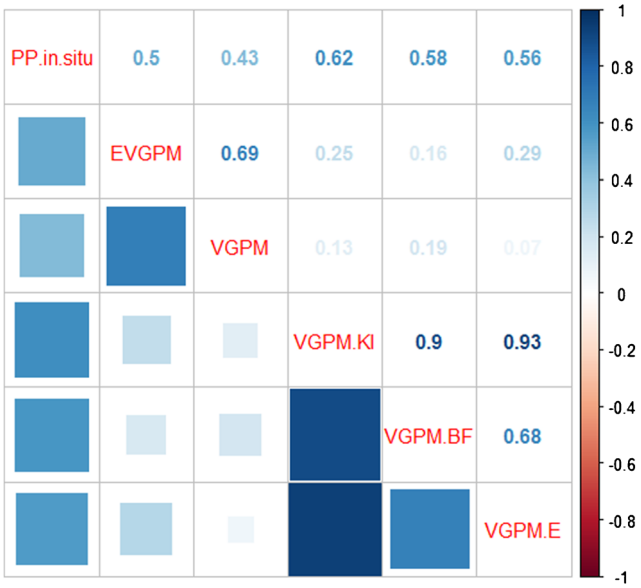

Figure 6. Correlation of PP measurements (mg C m^{-2} day^{-1}) between in-situ and various models in the region.

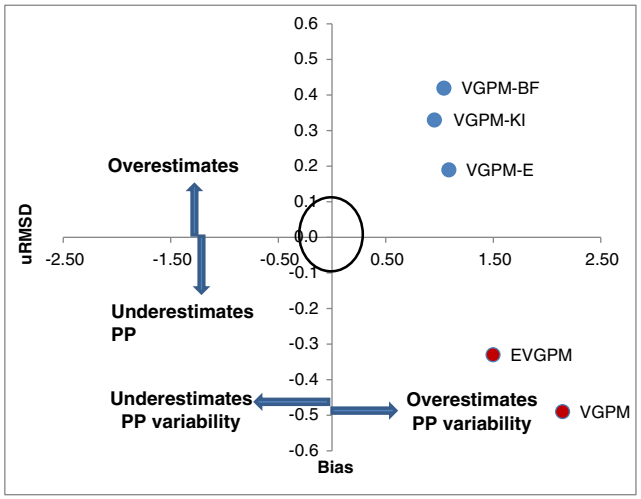

Figure 7. The ability of the different models represented in the Target diagram. The red symbols represent satellite PP estimates, and the blue symbols represent model PP values. The solid circle is the standard deviation of the observed data (σ_d) in the region.

the relation between VGPM-BF and P^B_{opt} by Kameda and Ishizaka (KI) with a data set in the eastern East China Sea. They observed that P^B_{opt} was underestimated when the temperature was high by both the models. The in-situ chlorophyll showed an inverse relationship with the P^B_{opt} in the current study, which was calculated by the KI variant of the VGPM model ($y = -0.101X + 4.296$, $R^2 = 0.686$). The range of in-situ temperature was higher, which was taken while estimating P^B_{opt} in the study region. The wider range of SST and better productivity because of convective mixing in the region could be the reason for the inverse relationship between P^B_{opt} and in-situ chlorophyll. A similar inverse relationship between P^B_{opt} and chlorophyll was observed from Sagami Bay and in open ocean data from the Pacific and Atlantic Ocean (Ishizaka et al. 2007).

Shang et al. (2010)estimated PP values in the Southern Ocean as 278 ± 187 mg C m^{-2} d^{-1} using the VGPM model. They attributed the difference in PP estimates primarily to the different phytoplankton physiology and the difference in the input variables. The large deviation between the satellite-based primary production algorithms was attributed primarily to the differences in the way they formulate primary production as a function of temperature. Tan and Guang-Yu 2009) examined the spatial and temporal variability of ocean primary productivity along the South China Sea using satellite primary production models. The maximum PP observed in the South China Sea was 374 mg C m^{-2} d^{-1} during winter with an overall mean of 308 mg C m^{-2} day^{-1}. In the present study region, in-situ PP ranged from 1937.8 to 4863.2 mg C m^{-2} d^{-1} (mean 3372.1 mg C m^{-2} d^{-1}). The PP values are comparatively higher than those reported in the South China Sea. Though both Arabian Sea and South China Sea are tropical marine ecosystem with comparable latitudinal expanse, the higher productivity in the former might be because of the unique physical,

Table 3. Validation statistics for each model in the region, i.e., Pearson correlation coefficient (r), MPE, root mean square error (RMSE), log Bias, *S* is the slope, *I* is the intercept of the linear regression coefficients, and R^2 is the coefficient of the determination.

In-situ vs	r	MPE	log_Bias	log_RMSD	ME	Slope (S)	Intercept (I)	R^2
EVGPM	0.500 (p<0.000)	46.36	0.14	0.02	− 4.19	0.453	116.77	0.251
VGPM	0.421 (p<0.000)	5.26	− 0.02	0.02	− 4.05	0.334	56.34	0.187
VGPM-KI	0.583 (p<0.000)	542.53	0.80	0.32	− 81.41	1.207	3045	0.383
VGPM-BF	0.548 (p<0.000)	659.55	0.89	0.40	− 101.29	1.553	3580	0.338
VGPM-E	0.531 (p<0.000)	367.97	0.66	0.22	− 55.62	0.963	1947	0.319

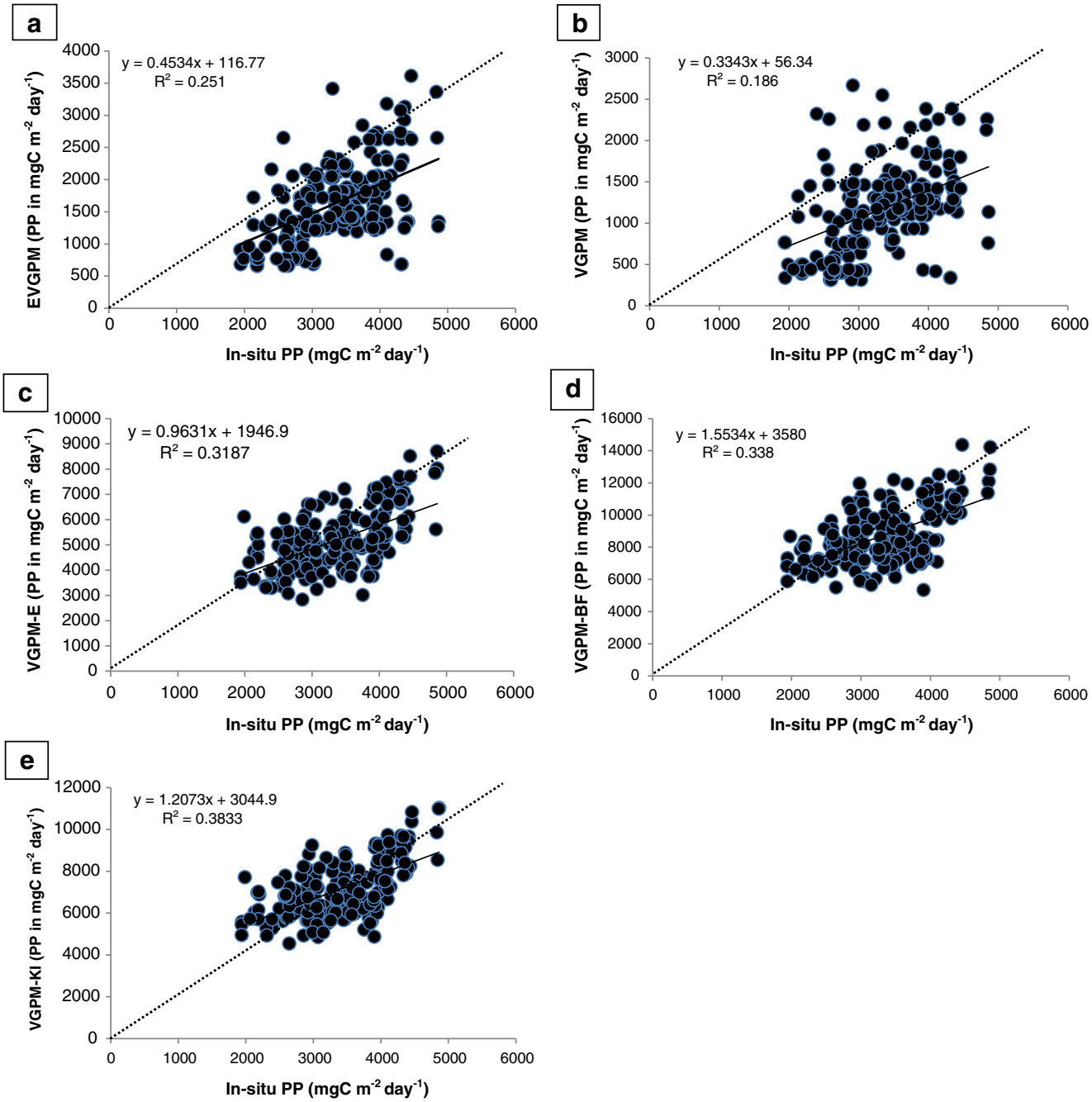

Figure 8. Scatter plots of log satellite, model and in-situ PP (mg C m^{-2} day^{-1}) in the northern Arabian Sea (N = 204). **a** EVGPM, **b** VGPM, **c** VGPM-E, **d** VGPM-BF, **e** VGPM-KI. Dotted line is the 1:1 line; the solid line is the linear regression.

biogeochemical environmental processes (nutrients, monsoon reversal, upwelling coastal currents, etc.).

The maximum fraction of model skill that may be attributable to uncertainties in both the input variables and in-situ NPP measurements was nearly 72%. Though the satellite-derived Chl-a and sea surface temperature adds to the uncertainties to the ocean color models, but is extremely challenging in the case of regions where typical variation in surface Chl-*a* occurs. In ocean color models, water column depth is a critical parameter and performed better in case I water than the case II waters (coastal waters) (Saba et al. 2011). The northern Arabian Sea is a highly productive ocean, and the study region is characterized as case II and coastal. In such cases, the application of conventional VGPM models are limited owing to erroneous estimation of P^B_{opt} and Z_{eu} by the embedded sub-models. Nevertheless, the use of in-situ input parameters in sub-models improves the model efficiency, making it applicable to present study region (Tripathy et al. 2012). The satellite-derived estimates for these coastal areas were highly erroneous, i.e., SST for the calculation of P^B_{opt}, Chl-*a*, k_d to calculate

Z_{eu}, etc. To address these uncertainties in the input variables, we adopted in-situ values in the algorithms. It was observed that the input variables (Chl-*a*, PAR, Z_{eu}, DL) together explained nearly 50% PP variability in the region. Among all the variables, chlorophyll-*a* was the most influential (p = 0.000), followed by DL (p = 0.003), and PAR (p = 0.007).

The average RMSD estimates for 12 ocean color models in the Northeast Atlantic Ocean region were 0.31 (Campbell et al. 2002) and 0.14 (Saba et al. 2010). The improvement of the model might be because of the larger sample size. The mean RMSD of 21 ocean color models tested in the tropical Pacific was 0.29 (Friedrichs et al. 2009), which was similar in skill to the Arabian Sea (0.22) and North Pacific Ocean (0.26). The average RMSD among the five models applied in the region was 0.10, which was better than the earlier discussed models and matching with previous values from Arabian Sea. Investigations by Campbell on the ocean color models in the eight regions revealed that the reduced model performance observed were characterized by High-Nitrate Low-Chlorophyll (HNLC), in the equatorial Pacific and the Southern Ocean (Campbell et al. 2002). The RMSD ranged from 0.02 to 0.10 across the different models attempted in the study region. The RMSD was low and best for the VGPM-E (RMSD is 0.02), and the VGPM-KI model (RMSD is 0.06), but higher values were noticed with satellite VGPM (RMSD is 0.14). The RMSD values estimated in the present study did not deviate from the earlier studies in the same region and other contemporary regions (Saba et al. 2010; Friedrichs et al. 2009), depicting the better model performance in the region.

The satellite-derived PP accounted for 50 to 80% of the variance in the in-situ PP, the rate of variation depending on the input parameters used in the model (Balch et al. 1992; Berthon and Morel 1992). The specific regional parameterization requires the development of various models to estimate the accurate PP to address the atypical optical and photophysiological characteristics from region to region (IOCCG 2000). The PP estimates by VGPM-KI model explained the highest variance of 38.3% in comparison with measured PP, but the lower variance was noticed with satellite PP data (25% variance by EVGPM and 19% variance with VGPM). The more variance in PP was explained by the modified models than global satellite models due to correction effect of in-situ input variables in the algorithm. The scatterplot depicted that the use of in-situ input variables (Chl-a and SST) in the modified models estimated PP (modeled PP) much higher than global satellite models (VGPM and EVGPM) and closer to the observed in-situ values of PP. Among the two satellite models, EVGPM performed better in the northern Arabian sea than VGPM. VGPM-KI and VGPM-E among modified models were found suitable for the studied region, which can be further improved through complete regional parameterization instead of a partial one which is attempted in the present study. We are in limitation with the estimation of some input variables (P^B_{opt}, Z_{eu}, and DL), which are crucial parameters in the algorithms. The results are in support that a regional approach should be adopted in interpreting ocean color satellite data in the Arabian Sea. We plan to strengthen the in-situ PP database (spatially and temporally) with advance methodologies to validate the global models, and to develop appropriate regional algorithms for future development and modelers to use in the applied research.

Summary and conclusion

The variability (monthly and seasonal) of primary production by the VGPM satellite data set was evident in the northern Arabian Sea (20–24°N, 66–72°E), majorly influenced by the oceanic-climatic parameters like sea surface temperature, light intensity, radiation which are higher than the global average. The primary production observed in the region was significantly higher when compared with other contemporary regions due to the efficient mixing of nutrients by convective winds during winter, coastal upwelling in monsoon season, and also because of the wider continental shelf. In-situ PP measurements are crucial to validate the global PP data sets with regional parameterization. In the present study, we validated global data sets (VGPM and EVGPM) with in-situ data. We also modified the existing global algorithms with the input parameterization (Chl-*a*, Z_{eu}, SST, etc.). We observed that the satellite data underestimated the PP as compared to the measured PP values, inferring that averaging of input parameters (SST, PAR, DL, Chl-*a*, Z_{eu}) at a global level across the ecosystems (polar to tropical and coastal to deep ocean) caused lower PP values by satellite equations. The input parameters explained over 40% variation in the measured PP, majorly by the Chl-*a*, SST, PAR, etc., but the complete in-situ parameterization has better explained the variations in measured PP. The modified models (with regional parameterization) performed better than the global satellite algorithms (VGPM and EVGPM) in the region. The model performance (RMSD and Bias) and efficiency values by the modified models in the region were better than the previous research findings. The modified models showed a fair correlation (r = 0.565 to 0.619) and regression (R^2 = 0.319 to 0.383) in addition to ME, bias, and RMSD than the satellite algorithms in the region. We were constrained to estimate only some input parameters (PAR, DL and P^B_{opt}) and coverage of the onboard sampling area. The complete regional parameterization and wider coverage during in-situ sampling will further improve the skill of the region based models and also evaluate the global algorithms.

Acknowledgements Authors are thankful to the Indian Council of Agricultural Research (ICAR), Dr. A. Gopalakrishnan, Director, ICAR-CMFRI, Scientist In-Charges & Scientists, Veraval Regional Centre and Dr. Sathianandan T.V., Head, Fishery Resources Assessment Division, ICAR-CMFRI, Kochi for the encouragement and support during the study period. The authors would like to thank Dr. Mini Raman, ISRO-Space Application Center, for the useful technical inputs about the study region.

Declarations

Conflict of interest The authors declare that they have no competing interests.

References

Arrigo KR, van Dijken GL, Bushinsky S (2008) Primary production in the Southern Ocean, 1997–2006. J Geophys Res Oceans 113: C08004. https://doi.org/10.1029/2007JC004551

Balch W, Evans R, Brown J, Feldman G, McClain C, Esaias W (1992) The remote sensing of ocean primary productivity: use of a new data compilation to test satellite algorithms. J Geophys Res Oceans 15 97(C2):2279–2293

Behrenfeld MJ, Falkowski PG (1997a) Photosynthetic rates derived from satellite-based chlorophyll concentration. Limnol Oceanogr 42(1): 1–20

Behrenfeld MJ, Falkowski PG (1997b) A consumer's guide to primary productivity models. Limnol Oceanogr 42:1479–1491

Behrenfeld MJ, O'Malley RT, Siegel DA, McClain CR, Sarmiento JL, Feldman GC, Milligan AJ, Falkowski PG, Letelier RM, Boss ES (2006) Climate-driven trends in contemporary ocean productivity. Nature 444:752–755

Berthon JF, Morel A (1992) Validation of a spectral light-photosynthesis model and use of the model in conjunction with remotely sensed pigment observations. Limnol Oceanogr 37:781–796

Boyd PW, Aiken J, Kolber Z (1997) Comparison of radiocarbon and fluorescence based (pump and probe) measurements of phytoplankton photosynthetic characteristics in the Northeast Atlantic Ocean. Mar Ecol Prog Ser 149:215–226

Campbell J, Antoine D, Armstrong R, Arrigo K, others (2002) Comparison of algorithms for estimating ocean primary production from surface chlorophyll, temperature, and irradiance. Glob Biogeochem Cycles 16(3):1035. https://doi.org/10.1029/2001GB001444

Carr ME, Friedrichs MA, Schmeltz M, Aita MN, Antoine D, Arrigo KR, Asanuma I, Aumont O, Barber R, Behrenfeld M, Bidigare R (2006) A comparison of global estimates of marine primary production from ocean color. Deep Sea Res Part II Top Stud Oceanogr 53: 741–770

DAHDF (2011) Report of the working group for revalidating the potential of fishery resources in the Indian EEZ. Department of Animal Husbandry & Dairying, Ministry of Agriculture New Delhi: 69.

De Sousa SN, Kumar MD, Sardessai S, Sarma VV (1996) Seasonal variability in oxygen and nutrients in the Central and Eastern Arabian Sea. Curr Sci 71:847–851

Doney SC (1996) A synoptic atmospheric surface forcing data set and physical upper ocean model for the U.S. JGOFS Bermuda Atlantic Time- Series Study (BATS) site. J Geophys Res 101:25,615–25, 634. https://doi.org/10.1029/96JC01424

Doney SC, Yeager S, Danabasoglu G, Large WG, McWilliams JC (2007) Mechanisms governing interannual variability of upper-ocean temperature in a global ocean hindcast simulation. J Phys Oceanogr 37:1918–1938. https://doi.org/10.1175/JPO3089.1

D'Ortenzio F, Iudicone D, de Boyer Montegut C, Testor P, Antoine D, Marullo S, Santoleri R, Madec G (2005) Seasonal variability of the mixed layer depth in the Mediterranean Sea as derived from in situ profiles. Geophys Res Lett 32: L12605. https://doi.org/10.1029/2005GL022463

Eppley RW (1972) Temperature and phytoplankton growth in the sea. Fish Bull 70:1063–1085

Eppley RW, Stewart E, Abbott MR, Owen RW (1987) Estimating ocean production from satellite-derived chlorophyll: insights from the Eastropac data set. Oceanol Acta SP:109–113

Falkowski P (1988) Ocean productivity from space. Nature 335:205

Friedrichs MA, Carr ME, Barber RT, Scardi M, Antoine D, Armstrong RA, Asanuma I, Behrenfeld MJ, Buitenhuis ET, Chai F, Christian JR (2009) Assessing the uncertainties of model estimates of primary productivity in the tropical Pacific Ocean. J Mar Syst 76:113–133

Gaarder T, Gran HH (1927) Investigations on the primary production of plankton in the Oso Fjord. Rapp Cons Explor Mar 42:48

Gouveia NA, Gherardi DFM, Wagner FH, Paes ET, Coles VJ, Aragao LEOC (2019) The salinity structure of the Amazon River plume drives spatiotemporal variation of oceanic primary productivity. J Geophys Res Biogeosci 124(1):147–165

Gregg WW (2008) Assimilation of SeaWiFS ocean chlorophyll data into a three-dimensional global ocean model. J Mar Syst:69, 205–225. https://doi.org/10.1016/j.jmarsys.2006.02.015

IOCCG (2000) Remote sensing of ocean colour in coastal and other optically-complex waters; Sathyendranath S (Eds) Reports of the International Ocean-Colour Coordinating IOCCG: Dartmouth, NS, Canada.

Ishizaka J, Siswanto E, Itoh T, Murakami H, Yamaguchi Y, Horimoto N, Ishimaru T, Hashimoto S, Saino T (2007) Verification of vertically generalized production model and estimation of primary production in Sagami Bay Japan. J Oceanogr 63:517–524

Joo H, Son S, Park JW, Kang JJ, Jeong JY, Lee CI, Kang CK, Lee SH (2016) Long-term pattern of primary productivity in the East/Japan Sea based on ocean color data derived from MODIS-aqua. Remote Sens 8:25

Kameda T, Ishizaka J (2005) Size-fractionated primary production estimated by a two-phytoplankton community model applicable to ocean color remote sensing. J Oceanogr 61:663–672

Kara AB, Wallcraft AJ, Hurlburt HE (2005) How does solar attenuation depth affect the ocean mixed layer? Water turbidity and atmospheric forcing impacts on the simulation of seasonal mixed layer variability in the turbid Black Sea. J Climate 18:389–409

Lan KW, Lian LJ, Li CH, Hsiao PY, Cheng SY (2020) Validation of a primary production algorithm of vertically generalized production model derived from multi-satellite data around the waters of Taiwan. Remote Sens 12:1627

Lobanova P, Tilstone GH, Bashmachnikov I, Brotas V (2018) Accuracy assessment of primary production models with and without photoinhibition using Ocean-Colour climate change initiative data in the North East Atlantic Ocean. Remote Sens 10:1116

Longhurst A, Sathyendranath S, Platt T, Caverhill C (1995) An estimate of global primary production in the ocean from satellite radiometer data. J Plankton Res 17:1245–1271

Malgorzata Stramska, Agata Zuzewicz (2013) Comparison of primary productivity estimates in the Baltic Sea based on the DESAMBEM algorithm with estimates based on other similar algorithms. Oceanologia 55:77–100

Manikannan R, Asokan S, Ali AH (2011) Seasonal variations of physico-chemical properties of the Great Vedaranyam Swamp, Point Calimere Wildlife Sanctuary, South-east coast of India. Afr J Environ Sci Technol 5:673–681

Mathew L, Pillai VN (1990) Chemical characteristics of the water around Andamans during late winter. Proc First workshop Scient Resul FORV Sagar Sampada:15–18

McClain CR (2009) A decade of satellite ocean color observations. Annu Rev Mar Sci **1**:19–42. https://doi.org/10.1146/annurev.marine.010908.16365

Morel A, Antoine D (2002) Small critters—big effects. Science 296: 1980–1982

Morel A, Berthon JF (1989) Surface pigments, algal biomass profiles, and potential production of the euphotic layer: relationships reinvestigated in view of remote sensing applications. Limnol Oceanogr 34:1545–1562

Morel A, Huot Y, Gentili B, Werdell PJ, Hooker SB, Franz BA (2007) Examining the consistency of products derived from various ocean color sensors in open ocean (Case 1) waters in the perspective of a multi-sensor approach. Remote Sens Environ 111:69–88

Murakami H, Sasaoka K, Hosoda K, Fukushima H, Toratani M, Frouin R, Mitchell BG, Kahru M, Deschamps PY, Clark D, Flora S (2006) Validation of ADEOS-II GLI ocean color products using *in-situ* observations. J Oceanogr 62:373–393

O'Malley R (2019) Ocean productivity. http://www.science.oregonstate.edu/ocean.productivity/ vgpm.model.php.

Pesce M, Critto A, Torresan S, Giubilato E, Santini M, Zirino A, Ouyang W, Marcomini A (2018) Modelling climate change impacts on nutrients and primary production in coastal waters. Sci. Total Environ 628:919–937

Peters M, Grant M, Halsall K (2019) Climate change initiative. http://www.esa-oceancolour-cci.org

Peterson BJ (1980) Aquatic primary productivity and the 14C-CO2 method: a history of the productivity problem. Annu Rev Ecol Evol Syst 11:359–385

Platt T, Caverhill C, Sathyendranath S (1991) Basin-scale estimates of oceanic primary production by remote sensing: The North Atlantic. J Geophys Res Oceans 96(C8):15147–15159

Racault MF, Le Quéré C, Buitenhuis E, Sathyendranath S, Platt T (2012) Phytoplankton phenology in the global ocean. Ecol Indic 14:152–163

Regaudie-de-Gioux A, Huete-Ortega M, Sobrino C, López-Sandoval DC, González N, Fernández-Carrera A, Vidal M, Marañón E, Cermeño P, Latasa M, Agustí S (2019) Multi-model remote sensing assessment of primary production in the subtropical gyres. J Mar Syst 196:97–106

Saba VS, Spotila JR, Chavez FP, Musick JA (2008) Bottom-up and climatic forcing on the worldwide population of leatherback turtles. Ecology 89:1414–1427

Saba VS, Friedrichs MA, Carr ME, Antoine D, Armstrong RA, Asanuma I, Aumont O, Bates NR, Behrenfeld MJ, Bennington V, Bopp L (2010) Challenges of modeling depth-integrated marine primary productivity over multiple decades: a case study at BATS and HOT. Glob Biogeochem Cycles 24(3). https://doi.org/10.1029/2009GB003655

Saba VS, Friedrichs MA, Antoine D, Armstrong RA, Asanuma I, Behrenfeld MJ, Ciotti AM, Dowell M, Hoepffner N, Hyde KJ, Ishizaka J (2011) An evaluation of ocean color model estimates of marine primary productivity in coastal and pelagic regions across the globe. Biogeosciences 8:489–503

Shang SL, Behrenfeld MJ, Lee ZP, O ' Malley RT, Wei GM, Li YH, Westberry T (2010) Comparison of primary productivity models in the Southern Ocean: preliminary results. Proc SPIE 7678 In Ocean Sensing and Monitoring II 7678:767808. https://doi.org/10.1117/12.853631

Siswanto E, Ishizaka J, Yokouchi K (2006) Optimal primary production model and parameterization in the eastern East China Sea. J Oceanogr 62:361–372

Smyth TJ, Tilstone GH, Groom SB (2005) Integration of radiative transfer into satellite models of ocean primary production. J Geophys Res Oceans 110(C10). https://doi.org/10.1029/2004JC002784

Strickland JDH, Parsons TR (1968) A practical handbook of seawater analysis. Bull Fish Ces Bd Canada 167:1–311

Tan S-C, Guang-Yu S (2009) Spatiotemporal variability of satellite-derived primary production in the South China Sea, 1998-2006. J Geophys Res 114(G03015). https://doi.org/10.1029/2008JG000854

Temkar GS, Azeez PA, Sikotaria KM, Brahmane VT, Metar SY, Gangan SS, Desai AY (2015) Correlation of phytoplankton density with certain hydrological parameters along the coastal waters of Veraval, Gujarat. J Marine Bio Assoc Ind 57:2

Thorsen S (2019) Sunrise and sunset calculator. https://www.timeanddate.com.

Tilstone G, Smyth T, Poulton A, Hutson R (2009) Measured and remotely sensed estimates of primary production in the Atlantic Ocean from 1998 to 2005. DEEP-SEA RES PT II 56:918–930

Tilstone GH, Taylor BH, Blondeau-Patissier D, Powell T, Groom SB, Rees AP, Lucas MI (2015) Comparison of new and primary production models using SeaWiFS data in contrasting hydrographic zones of the northern North Atlantic. Remote Sens Environ **156**: 473–489

Tripathy SC, Ishizaka J, Siswanto E, Shibata T, Mino Y (2012) Modification of the vertically generalized production model for the turbid waters of Ariake Bay, southwestern Japan. Estuar Coast Shelf Sci 97:66–77

Vase VK, Dash G, Sreenath KR, Temkar G, Shailendra R, Koya KM, Divu D, Dash S, Pradhan RK, Sukhdhane KS, Jayasankar J (2018) Spatio-temporal variability of physico-chemical variables, chlorophyll a, and primary productivity in the northern Arabian Sea along India coast. Environ Monit Assess 190:148

Yamada K, Ishizaka J, Nagata H (2005) Spatial and temporal variability of satellite estimated primary production in the Japan Sea from 1998 to 2002. J Oceanogr B:857–869

Zainuddin M, Kiyofuji H, Saitoh K, Saitoh SI (2006) Using multi-sensor satellite remote sensing and catch data to detect ocean hot spots for albacore (*Thunnus alalunga*) in the northwestern North Pacific. DEEP-SEA RES PT II **53**:419–431